Biomaterials and Medical Applications

Research Article A SCITECHNOL JOURNAL

Preparation and Characterization of Metal and Metal Oxide Nanoparticles Embedded Composite Polymer Films from Chitosan and Guar Gum for Biomedical and Packaging Applications

K Subramanian* and Shri Poornima R

Department of Biotechnology, Bannari Amman Institute of Technology, Sathyamangalam, Tamil Nadu, India

***Corresponding author:** K Subramanian, Department of Biotechnology, Bannari Amman Institute of Technology, Sathyamangalam, Tamil Nadu, India, Tel: +9003135462; E-mail: drksubramanian@rediffmail.com

Received date: 14 June, 2022, Manuscript No. BMA-22-66643;

Editor assigned date: 17 June, 2022, PreQC No. BMA-22-66643 (PQ);

Reviewed date: 01 July, 2022, QC No. BMA-22-66643;

Revised date: 06 September, 2022, Manuscript No. BMA-22-66643 (R);

Published date: 13 September, 2022, DOI: 10.4172/2577-0268.1000505

Abstract

Chitosan/Guar gum based films have established significant consideration in medical and packaging applications. However, the mechanical properties of CS-GG films required improvement for broadening their applications in the above areas. To confront these challenges, nanoparticles were prepared and used as fillers to modify the property of CS-GG films. After incorporating the nanoparticles, the polymer films become more amorphous, as revealed by XRD. The approximate average particle size calculated from the SEM picture was less than 500 nm. The surface features of CS-GG films analyzed through SEM indicated partial agglomerations of nanoparticles. Comparison of NH_2 and OH stretching frequency of composite film with those of films obtained from pure polymer indicated that there might be possible H-bonding interaction between functional groups like NH_2 and OH in the composite film. The ZnONPs and AgNPs embedded polymer films showed an increase in tensile properties, unlike CuONP-loaded polymer films. The latter may be due to comparatively less dispersibility in the polymer matrix, which is amorphous. The tensile strength of AgNP loaded and ZnONP loaded films increased by 26.69% and 30.39%, but in CuONP film, it decreased due to the poor dispersibility of cuONPs. An unusual correlation has been observed between Tensile strength and Elongation. TGA analysis of the thermo grams of the films revealed that the onset degradation temperature of NPs loaded films decreased compared to unloaded films. These may be due to the catalytic nature of NPs and pure thermal degradation. There is no significant change in the onset temperature of metal oxide NPs films. However, the stability of the films at a temperature beyond onset degradation temperature improved. The antimicrobial assay studies using *E. coli* and *B. subtilis* revealed the zone of inhibition, indicating the films are antimicrobial agents. The water vapour permeability test indicated that the films become less water vapour permeable. The films maintained their structural integrity, as revealed by the water immersion test. These improved properties of functional bio polymers show great potential as food packaging materials and other biomedical applications.

Keywords: Metal and metal oxide nanoparticles; Composite film; Solution casting; Tensile strength; Morphology; Water vapour permeability; XRD; FTIR; SEM; TGA

Introduction

Metal and metal oxide nanoparticles embedded composite films prepared from various biopolymers such as chitosan, sodium alginate, agar-agar, carboxy methyl cellulose, guar gum; starch, gelatin and chitosan are widely employed for the various biomedical applications such as scaffolding in tissue engineering, food and non-food packaging applications instead of the synthetic polymers. Preparation of these films with electrical conductivity, resistance to moisture permeability and air, good mechanical properties such as tensile strength, tear strength, flexibility etc. The purpose of imparting conductivity to the film is to make it more biocompatible in scaffold applications and eliminate static charge in packaging applications. While making the composite films, additives such as glycerol, polyvinyl alcohol, citric acid and polyethene glycol are added in appropriate quantities to make the film flexible and increase nanoparticle stability. Various applications of these films include electrochemical biosensors, plasmonic hydrogen detection etc. In this direction, in the present investigation, a composite film from the widely and cheaply available biopolymers such as Chitosan and guar gum will be fabricated by incorporating copper oxide, zinc oxide as well as silver nanoparticles separately and characterize for antimicrobial properties, thermal properties, swellability, tensile strength, morphology and structure by FTIR for biomedical and other applications. The nanoparticles will be synthesized by chemical method either *in-situ* during the film casting or prepared separately and dispersed in the solution for casting the film.

Chitosan is an abundant biopolymer, an N-deacetylated chitin derivative containing β-1-4 linked 2-amino-2-deoxy-D-glucopyranose. The hunt for biodegradable and non-toxic materials to balance the consumption and production of plastics for the food industry has led to research on edible polysaccharide films, including Chitosan, the crustacean derived amino polysaccharide. Chitosan films have beneficial properties like high antimicrobial properties, flexibility, strength, and water permeability resistance, which led to the development of polymeric nanoparticle film in food packaging and biomedical applications. Despite these outstanding qualities, chitosan has weak mechanical and barrier properties, which can limit its application. To counter this limitation, reinforcement materials such as nanoparticles are commonly utilized. Chitosan has amine ($-NH_2$) and hydroxyl (-OH) groups in its structure, forming complexes with various nanomaterials, including metal nanoparticles and oxide agents, resulting in a reinforced material [1].

Guar gum is a novel agrochemical derived from cluster bean endosperm. Guar gum powder is widely used as an additive in the food, pharmaceutical, paper, textile, explosive, oil well drilling, and cosmetics industries. Guar gum's most unique property is its ability to rapidly hydrate in cold water systems to produce highly viscous

solutions. Guar gum forms a viscous colloidal dispersion, a thixotropic rheological system when completely hydrated. Guar gum based films have exceptional mechanical strength, improved barrier properties and antimicrobial or microbe resistance. Fabricating films based on pea starch guar gum bio composite edible films has revealed that these edible films were used as active agents in food packaging applications. Furthermore, the solvent casting method makes guar gum/Ag-Cu nano composite films. Because of its excellent thermo mechanical, antibacterial and O_2 barrier properties, used as an active food packaging material [2,3].

Polyvinyl Alcohol (PVA) is a hydroxyl rich biocompatible polymer that is non-toxic, semi-crystalline, and water soluble. It is widely utilized in the food packaging industry. Due to its characteristics, it is used in the building and home sectors, such as biocompatibility, mechanical strength, and solvent compatibility resistance. The limitations of using PVA in food packaging are poor biodegradation rate and high absorption of moisture content. As a result, it is frequently combined with biopolymers and bio based materials to boost performance and reduce environmental impact properties. Also, Mechanical and electrical constraints on PVA film properties and water permeability are removed by incorporating various nano materials or combining them with different biopolymers [4].

Copper Oxide (CuO) is broadly employed in various industries, including catalysts, ceramics, and thermo electrics superconducting, sensors, glass superconducting materials and antimicrobial agents. Production of CuO-NPs is less expensive when compared to gold and nanoparticles of silver. Because of their powerful antibacterial properties, distinctive crystal structure, physical and chemical properties size, aggregation state in liquids and other features of NP play an essential part in the final interactions of NPs with target cells. CuO-NPs were reported to have potent antimicrobial activity against *Escherichia coli* and *Bacillus*, depending on the concentration and particle size.

ZnO NPs are a type of nanomaterial that may be employed to improve mechanical and chemical properties and bioactivity. When applied to food packaging materials, ZnO NPs have been shown to boost antibacterial activity, mechanical strength and barrier characteristics. Including ZnO NPs improves the barrier characteristics of chitosan films by creating complex routes that make the passage of water or oxygen through the polymeric chain more challenging after the NPS fills the porous areas within the macromolecule structure.

Silver nanoparticles are essential nanoparticles regarded as novel chemicals combined into a polymer matrix to develop revolutionary nano composite materials in food packaging (AgNPs). Furthermore, AgNPs have antibacterial capabilities against various pathogens, including bacteria, yeast and mould. As a result, using such materials in the food sector could help increase the shelf life of food goods by reducing rotting and pathogenic microorganisms.

The benefits of silver nanoparticles in edible packaging include negligible effects on food sensory qualities and their excellent antibacterial activity. This packaging does not harm food goods sensory characteristics and customers find it more acceptable. Natural chemicals, on the other hand, are frequently employed [5].

Materials and Methods

Materials

Polymers like guar-gum, chitosan and chemicals like copper sulphate, silver nitrate, acetic acid, sodium hydroxide, sodium borohydride and cross linker citric acid. Plasticizers glycerol and stabilizing agents like polyvinyl alcohol were obtained from Hi-Media laboratories, Bannari Amman institute of technology, Sathyamangalam laboratory.

Methods

Synthesis of CuO nanoparticles by precipitation method

CuO nanoparticles were obtained by precipitation of copper sulphate pentahydrate and sodium hydroxide. Copper sulphate pentahydrate (0.01 M) was prepared in distilled water and sodium hydroxide (0.1 M) solution was prepared and gradually added under constant stirring up to pH 14 to yield a black precipitate. The precipitate was centrifuged, washed thrice with distilled water, and dried at 80°C in a hot air oven.

Synthesis of ZnO nanoparticles by precipitation method

ZnO nanoparticles were obtained by precipitation of Zinc sulphate and sodium hydroxide. Zinc sulphate (0.01 M) was prepared in distilled water and sodium hydroxide (0.1 M) solution was prepared and gradually added under constant stirring to yield a white precipitate. The precipitate was centrifuged, washed thrice with distilled water and dried at 80°C in a hot air oven.

Synthesis of Ag nanoparticles by *in situ* chemical synthesis

Ag nanoparticles were obtained by *in situ* precipitation of silver nitrate and sodium borohydride. Silver nitrate (0.002 M) solution (25 ml) was prepared in distilled water. To that, 0.5 ml of ammonia was added and sodium borohydride (0.002 M) solution ice cold (25 ml) was prepared and gradually added to the polymer blend under constant stirring to yield a yellowish orange precipitate [6].

Preparation of CuO, ZnO and Ag nanoparticles Chitosan/ Guar gum bio nano composite films

Different concentrations of chitosan/guar gum were prepared by solution casting method. Chitosan and guar gum solutions (0.5%w/v) were prepared separately and then mixed in the ratio of 1:1(v/v). The prepared CuO-NPs, ZnO-NPs, and Ag-NPs were prepared and 2% were added to the prepared polymer blend solutions. The three different compositions of the polymer solution were sonicated for three h at 25°C, 500 W, frequency, 20 kHz and amplitude of 50% using a sonicator. The polymer with CuO, ZnO and Ag bio nano composites solutions was transferred into a transparent glass plate and left at room temperature for 3-4 days to vaporize the solvent. To remove excess glycerol or moisture from the film, ethanol or methanol was sprayed and dried in a vacuum oven.

Preparation of Chitosan/Guar gum bio nano composite films without nanoparticles

Different concentrations of Chitosan/Guar gum were prepared by solution casting method. Chitosan and guar gum solutions (0.5%w/v)

were prepared separately and then mixed in the ratio of 1:1 (v/v). The polymer bio-nano composites solutions were transferred into a transparent glass plate and left at room temperature for 3-4 days to vaporize the solvent. To remove excess glycerol or moisture from the film, ethanol or methanol was sprayed and dried in a vacuum oven.

Characterization of Chitosan/Guar gum bio nano composite films

X-Ray Diffraction pattern (XRD): The prepared nanoparticle embedded polymer films were evaluated in X-ray diffractometer shimadzu model XRD 6000 using Cu Ka radiation (40 kV, 30 mA, with λ=0.15418 nm) with scans were run in the range of a 2q from 5 to 80°C with a scanning speed of 10.0000 (deg/min) and preset time of 0.60 (sec). The d-spacing was calculated in the diffraction patterns using Bragg's equation (nλ=2d sin q).

Morphological characterization: The morphology of the nano composite film samples was analyzed on surfaces of the prepared nano composite films and examined using Scanning Electron Microscopy (SEM) JEOL JSM 6390, operated at 10 kV, with a maximum magnification of 300 × and a resolution until 2 nm [7,8].

FT-IR spectra: The interactions in fabricated bio nano composites were assessed by FT-IR spectra using (shimadzu iraffinity-1s) FT-IR spectrophotometer using miracle10 single reflectance Attenuated Total Reflection (ATR) accessory. The internal reflection element was a single reflection zinc selenide (ZnSe) crystal. FTIR spectra were recorded with 4 cm^{-1} resolution and 45 scans on average to obtain a good signal to noise ratio. The ATR measurement area was a circular spot of approximately 1.5 mm diameter prism. The samples were kept directly on the ZnSe prism and the spectrum was recorded in the wavenumber range 400-4000 cm^{-1}.

Thermogravimetric analyzer: The thermal stability of films was characterized by a Q50 TGA analyzer. Films were heated from 10°C to 550°C at a rate of 10°C/min in a nitrogen atmosphere (100 mL/min).

Breaking load: The tensile strength of the nano composite films was measured with universal testing machine dak inc at a speed of 10 mm/min. Each film was cut into pieces with dimensions of 8 cm × 5 mm. Four films were measured to obtain the average values for each film and compare the tensile strength of each film [9].

Swellability of film in water: The four films were put in water to test the swellability of films. The films were dried and did not dissolve in water.

Moisture absorption of films: Four bio nano composite films were immersed in distilled water at 3 hrs intervals for three days. The initial and final weight (after drying) was measured to calculate the swellability of the films.

Water vapour permeability: Dry fruits, flour were packed inside the film and sealed. They were kept in a desiccator containing water for three days intervals. After three days, the weight was checked to determine the water vapour permeability.

Antimicrobial activity of the films: The antimicrobial assay of nanoparticle embedded polymer films was carried out using the disc diffusion method. 0.1 mL of gram positive bacteria *Bacillus subtilis* and gram negative bacteria *E. coli* strains were spread on the surface of the plate containing Muller Hinton agar media. After that, the films were cut into pieces, placed on the plates and incubated at 37°C for 24 hrs to get the clearance zone. After incubation at 37°C/24 hrs, the diameter of the clear inhibition zone surrounding the wells was measured [10-12].

Results and Discussion

X-Ray Diffraction pattern (XRD)

XRD analyzed the crystalline phase of the samples as a non destructive approach. X-ray patterns of Ch/GG/CuO, Ch/GG/ZnO, Ch/GG/Ag, and Ch/GG bio nano composites were reported here, as shown in Figure 1. The firm peaks of CuO nanoparticles located at 2θ=38.84°, 35.70°, 49.0825° are assigned to (101), (011), (110) plane orientation of joint committee on powder diffraction standards (48-1548). The prominent crystalline peaks of CuO nanoparticles embedded polymer film located at 2θ=21.3, 22.68, 20.0° are assigned to (101), (011), (110) plane orientation of the joint committee on powder diffraction standards (48-1548) [13]. The most substantial crystalline peaks were broadly attributed to the predominant amorphous nature of polymers and are observed in CuO NP separately but not in CuONP embedded polymer film. The prominent crystalline peaks of ZnO nanoparticles embedded polymer film located at 2θ=21.15°, 10.70°, 34.7750° are assigned to (101), (011), (110) plane orientation of joint committee on powder diffraction standards (043-00027). The prominent crystalline peaks of ZnO nanoparticles located at 2θ=9.2828°, 33.4921°, 35.9° are assigned to (101), (011), (110) plane orientation of the joint committee on powder diffraction standards (043-00027) [14]. The most substantial crystalline peaks were broadly attributed to the predominant amorphous nature of polymers observed in ZnO NP separately and in ZnONP embedded polymer film. The prominent crystalline peaks of Ag nanoparticles embedded polymer film located at 2θ=20.95°, 16.90°, 14.3432° are assigned to (101), (011), (110) plane orientation of joint committee on powder diffraction standards (04-0783). The most substantial crystalline peaks were broadly attributed to the predominant amorphous nature of polymers observed in AgNP separately and also observed in AgNP embedded polymer film.

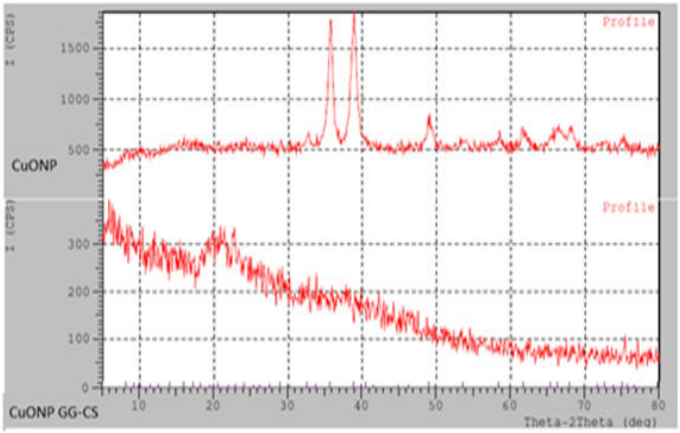

XRD diffraction patterns of CuONP and CuONP embedded GG-CS composite film

a

Figure 1a: XRD DIFFRACTIONS PATTERNS OF CuONP and CuONP embedded GG-CS films.

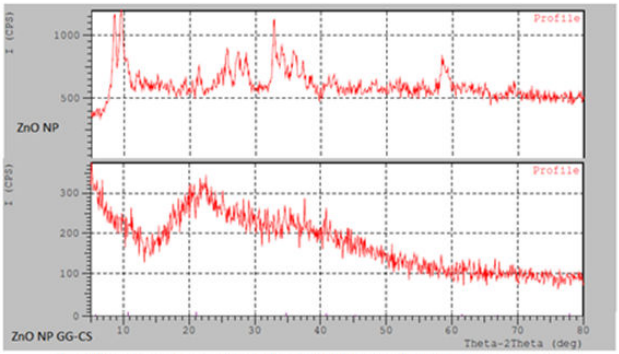

b

Figure 1b: XRD DIFFRACTIONS PATTERNS OF ZnONP and ZnONP embedded GG-CS films.

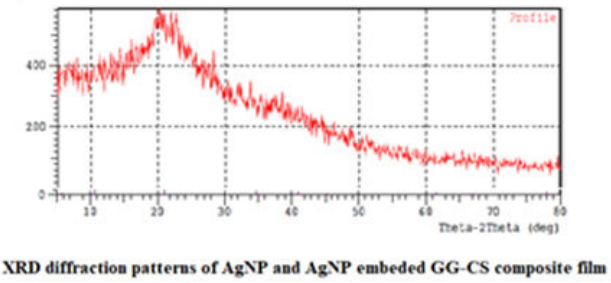

c

Figure 1c: XRD DIFFRACTIONS PATTERNS OF AgNP and AgNP embedded GG-CS films.

SEM examination of the prepared bio nano composites

The morphology of CuO-NPs, ZnO-NPs, AgNPs, Ch/GG blend and the prepared films were evaluated using SEM (Scanning Electron Microscope). The particle diameter of different particles was measured using Image. The particle diameter for GG-CS CuoNP film is 5 µm at the highest resolution of 3000 and 10 kV. The CuONPs are evenly distributed throughout the film. The CuONPs had spheres shaped as depicted in the Figure 2. The GG-CS CuONP film has a rough rectangular surface indicating compatibility between the polymers. In ZnONP embedded film, the particle diameter of two horizontal particles is 2 µm at the highest resolution of 5500, 10 kV frequency and are not homogenous but seem heterogeneous. This reveals the agglomeration of particles due to GG-CS. The GG-CS ZnONP film has irregular shapes due to GG-CS agglomeration, indicating the polymers' immiscibility. In AgNP embedded film, the particle diameter is 5 µm at the highest resolution of 3000 and 10kV frequency and there is an agglomeration of polymers due to the immiscibility of GG-CS. The small particles are Silver nanoparticles dispersed all over the film with a particle diameter of 0.514 µm. Different particle sizes, including 0.515 µm and 0.615 µm, are measured. The particles are irregular in shape with a heterogeneous distribution. Figure 2 shows the dispersion of particles in the polymer film with a 2% addition of each nanoparticle in the film [15].

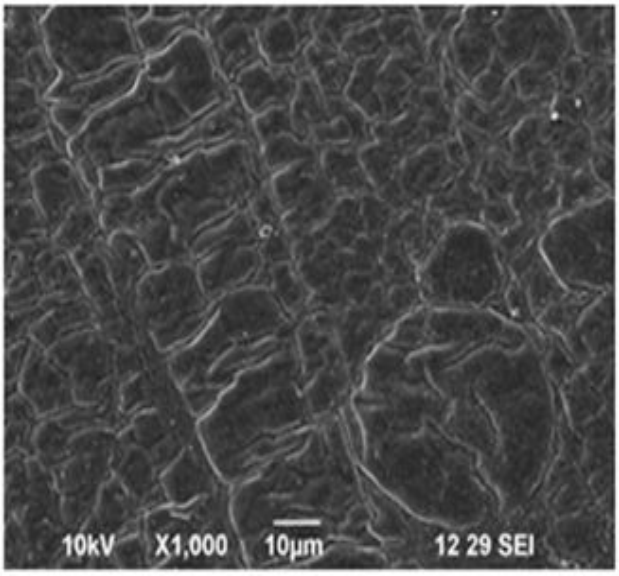

a

Figure 2a: SEM image of CuONP CS-GG film.

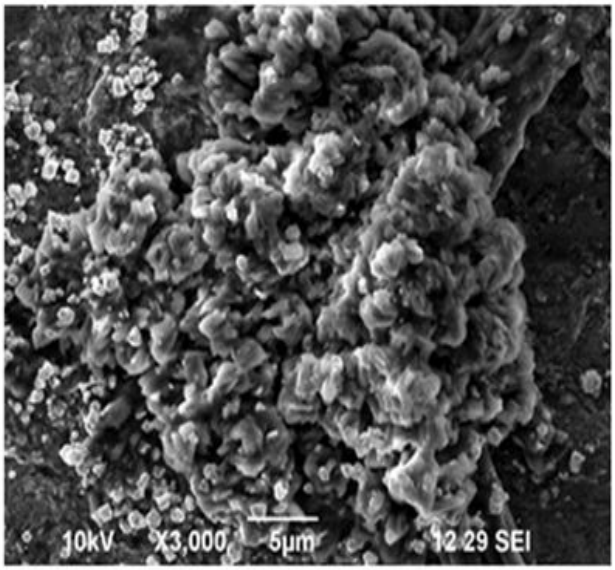

b

Figure 2b: SEM image of ZnONP CS-GG film.

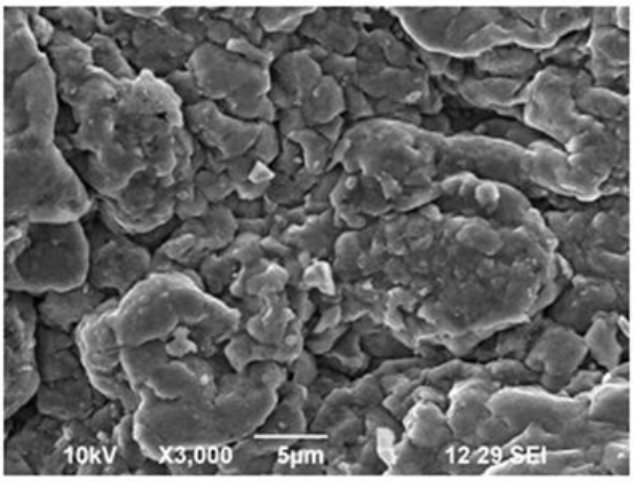

c

Figure 2c: SEM image of AgNP CS-GG film.

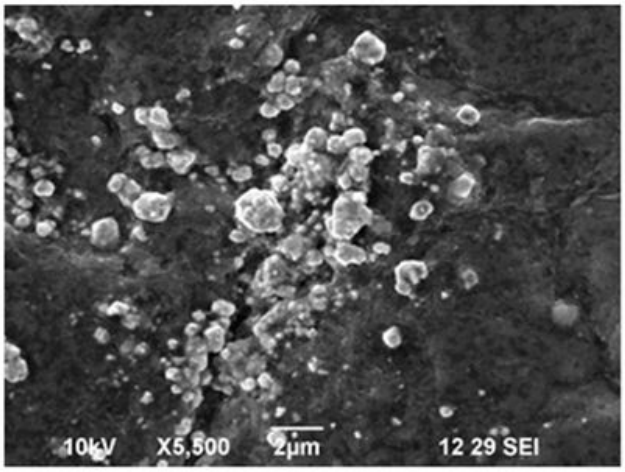

d

Figure 2d: SEM image of CS-GG film.

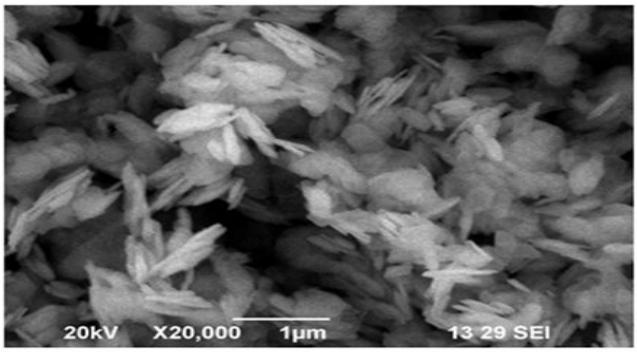

e

Figure 2e: SEM image of ZnONP.

FT-IR spectroscopy

FT-IR spectroscopy is one of the most superior approaches to recognizing functional groups in a molecule to establish possible intermolecular interactions among various constituents in the nano composite polymer films. From Figure 3, in CuO nanoparticles embedded polymer film, the broad and strong absorption band was observed around 3294.42 cm^{-1} attributable to free and bound O-H groups, which formed hydrogen bonding with a carboxylic acid in the polymer and CuO nanoparticles film. The weak and broad absorption band observed around 2926.01 cm^{-1} attributed to the O-H group, which formed hydrogen bonds with the hydroxyl group with the polymer and CuO nanoparticles film. The peaks at 1612.49, 1562.34, 1537.27, 1305.81 and 1265.30 cm^{-1} were assigned to C=C stretching, N-O stretching and C-O stretching, which had medium and strong interaction forms of ester linkage and alkene linkage which attributes bonding of the polymer to CuO nanoparticles. CuO vibrational bands had absorption spectra at 470.63 cm^{-1}. These interactions determined composite films mechanical properties and hydrophobicity, attributed to the effects of hydrogen bonds [16].

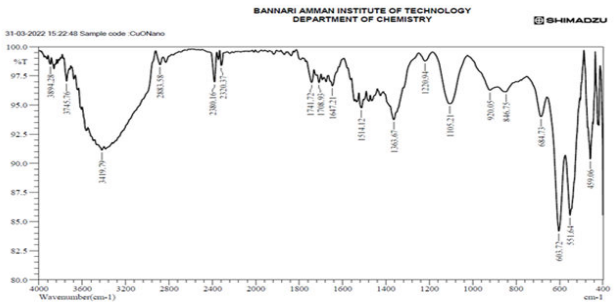

a

Figure 3a: FTIR spectrum of CuONP.

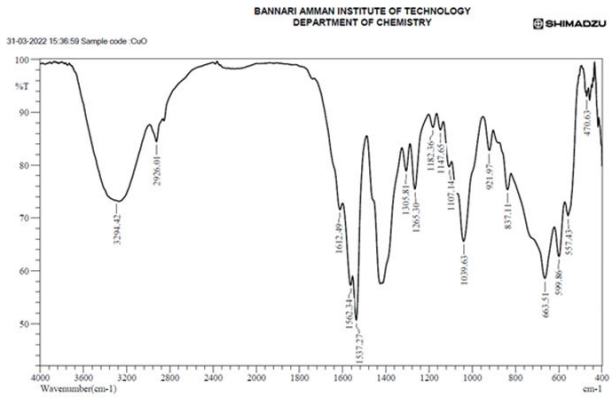

b

Figure 3b: FTIR spectrum of CuONP embedded CS-GG film.

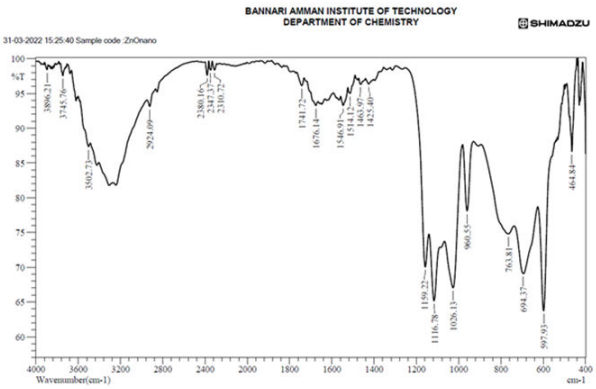

c

Figure 3c: FTIR spectrum of ZnONP.

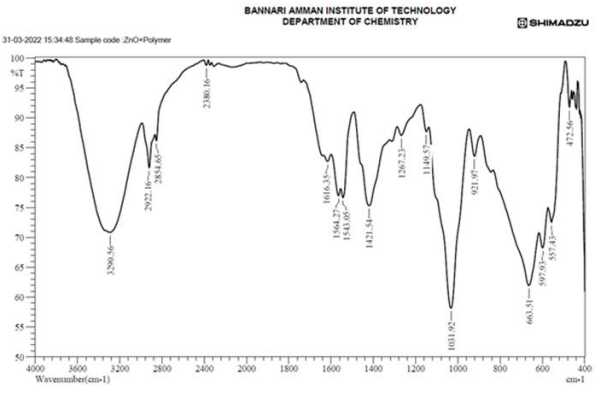

d

Figure 3d: FTIR spectrum of ZnONP embedded CS-GG film.

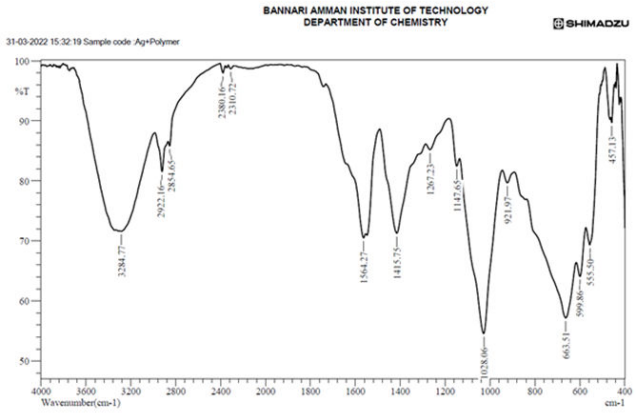

Figure 3e: FTIR spectrum of AgNP embedded CS-GG film.

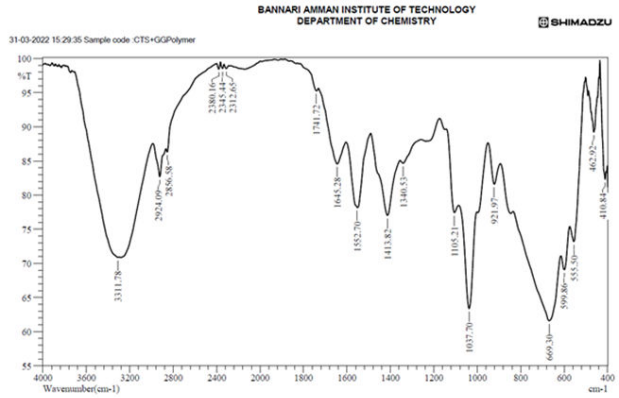

f

Figure 3f: FTIR spectrum of CS-GG film.

In ZnO nanoparticle embedded polymer film, the medium sharp absorption spectra were observed at 3290.56, with OH stretching indicating hydroxyl group of Ch/GG. At the peak 2922.16 and 2854.65, the absorption spectra were strong and broad with the carboxylic acid functional group in the Ch/GG. The absorption spectra 2380.16 had vigorous O=C=O stretching attributed to the carbon dioxide group. The peaks at 1616.35, 1564.27, 1543.05, 1421.54, 1267.23, 1149.57, and 1031.92 have medium and strong interactions assigned to C=C stretching, N-O stretching, O-H bending, C-N stretching, C-O stretching formed amine linkages and alkene structures. The absorption spectra from 663.51, 597.93, 557.43, and 472.56 are where the Zn-O bands are formed, indicating the ZnO-Ch/GG linkage [17–20].

In Ag nanoparticle embedded polymer film, the strong, broad spectra were observed at 3284.77, 2922.16, with O-H stretching indicating the presence of hydroxyl group in Ch/GG. The absorption spectra at the peak with wavenumbers 2380.16 and 2310.72 has strong O=C=O stretching attributing to the carbon dioxide group in Ch/GG complex. The peaks at 1564.27, 1267.23, 1147.65 and 1028.06 have strong and medium interactions with C=C stretching, O-H bending, and C-O stretching, attributing to functional groups alcohol, ester and ether linkages. The absorption spectra from 663.51, 599.86, 555.50

and 457.13 are where the Ag-Ch/GG bands are formed, indicating the presence of Ag nanoparticles.

Comparing three different nanoparticles embedded polymer films, the Cu-O, Zn-O and Ag nanoparticles bonded with Ch/GG at the lowest wavenumbers indicating the flexibility and stability of the nano composite films.

Thermo gravimetric analysis

The thermal stability of nanoparticle-embedded Ch/GG films was investigated using Thermo Gravimetric (TG) and Derivative Thermo Gravimetric (DTG). From Figure 4 in CS-GG control and NP loaded films, the TG and DTG were achieved in four steps in the temperature range of 100–550°C. The first step was from room temperature to 120°C and corresponded to film water loss. The second step of 120°C to 200°C was due to glycerol degradation. The degradation rate of films appeared between 180°C and 550°C and was attributed to the decomposition of the nanoparticles embedded in Ch/GG films. In CS-GG-PVA and Physical blend GG-CS, the TG and DTA were achieved in four steps in the temperature range of 100–550°C. The first step was from room temperature to 120°C and corresponded to water loss in polymers. The second step of 120 °C to 300°C was due to glycerol degradation. The degradation rate of films appeared between 150°C and 550°C and was attributed to the decomposition of the Ch/GG/PVA films and the physical blend of CS/GG. In CS-GG control films with and without NP loaded films, the TG and DTA were achieved in four steps in the temperature range of 100–550°C. The first step was from room temperature to 180°C and corresponded to film water loss. The second step of 120°C to 250°C was due to glycerol degradation. The degradation rate of films appeared between 310°C and 550°C and was attributed to the decomposition of the nanoparticles embedded in Ch/GG films and without NP CH/GG films. In CS/GG/PVA, the TG and DTG were achieved in four steps in the temperature range of 100–550°C. The first step was from room temperature to 180°C and corresponded to the no water loss in the polymer. The degradation rate of films appeared between 300°C and 550°C and was attributed to the decomposition of the CS/GG/PVA polymers.

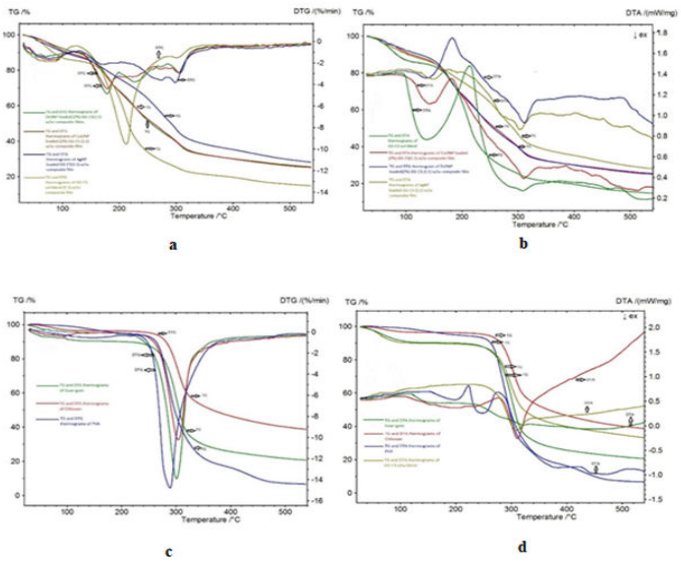

Figure 4: Thermograms of CS-GG films with and without nanoparticles. a) TG and DTG thermograms of CuO, ZnO, Ag nanoparticles loaded CS-GG films and without nanoparticles loaded CS-GG film; b) TG and DTA thermograms of CuO, ZnO, Ag nanoparticles loaded CS-GG films and without nanoparticles loaded CS-GG film; c) TG and DTA thermograms of GG, CS, PVA, GG-CS phy blend; d) TG and DTG thermograms of GG, CS, PVA.

Antimicrobial property

The zone of inhibition shows the antimicrobial activity of CuO-NP-Ch/GG, ZnO-NP-Ch/GG, and Ag-Ch/GG due to the good diffusion method. The zone of inhibition from Figure 5 was found in Ag/Ch/GG with a diameter of 0.5 mm in both *E. coli* and *B. subtilis* strains. The Ag/Ch/GG inhibited both the strains with greater clearance than CuO/Ch/GG and ZnO/Ch/GG. This shows that Ag nanoparticle embedded polymer films have a greater capacity for inhibiting microorganisms. Hence, this film can be preferred more in food packaging and biomedical applications.

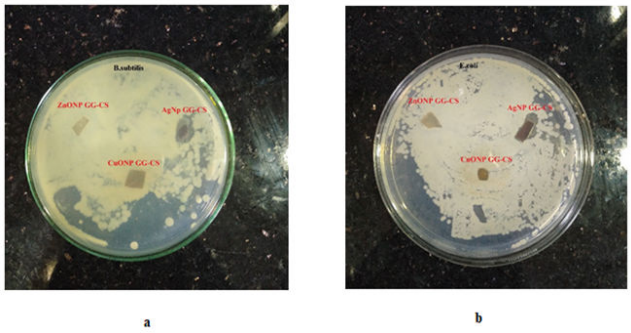

Figure 5: Antimicrobial assay. a) Anti-microbial activity in *B. subtilis*; b) Anti-microbial activity in *E. coli.*

Breaking load of the film

The tensile strength and the breaking load of the samples are measured by UTM (Universal Testing Machine Dak system Inc). The physical and mechanical properties of the bio nano composite films must be significant to determine their application as packaging materials. The Tensile Strength (TS), breaking load at elongation (EB), and young's modulus (E) of the CS-GG NP based films were analyzed. Figure 6f shows the peak load of CS-GG Ag films was 3.9442 N with the highest tensile strength of 2.6295 N/sqmm and elongation at break of 26.6199%. This depicts the flexibility and elasticity of the films with Ag nanoparticles. However, the CS-GG solution blend film had a peak load of 2.9316 N with the highest tensile strength of 2.3453 N/sq.mm and elongation break at 26.200 %, making it less flexible when compared to Cs-GG AgNP film. The Cs-GG ZnONP films had a tensile strength of 5.6749 N/sq.mm and a peak load of 4.3533 N with an elongation break at 30.3988%, which is the highest. The Cs-GG CuONP films had a peak load of 3.8606 N with the highest tensile strength of 3.3570 N/Sq.mm and elongation break percentage of 14.600%, which is the least when compared to other films. Therefore, Cs-GG AgNP and CS-GG ZnONP films have greater tensile strength and elongation with enhanced flexibility than the CS-GG solution blend. Hence, these films are preferred in food packaging and other biomedical applications (Table 1).

a

Figure 6a: UTM Universal Testing Machine Dak system Inc at KCT.

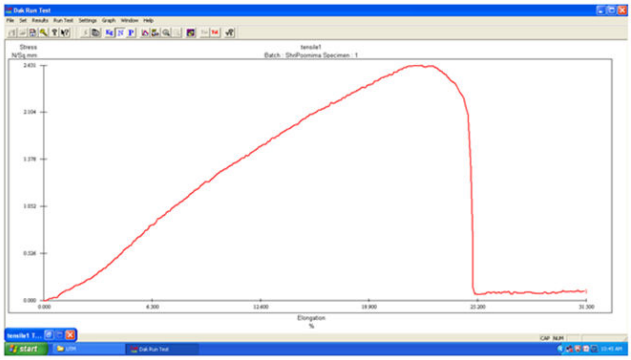

b

Figure 6b: Stress-Strain curve of CS-GG AgNP Film 1.

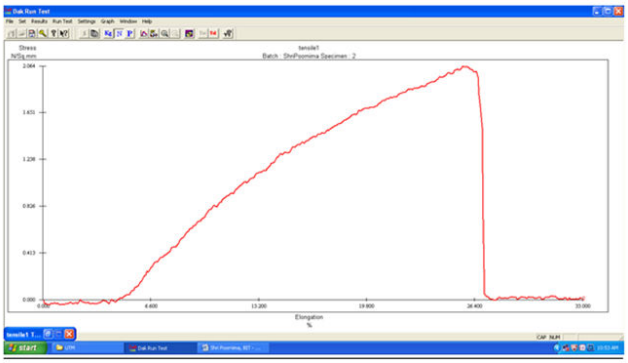

c

Figure 6c: Stress-Strain curve of CS-GG AgNP Film 2.

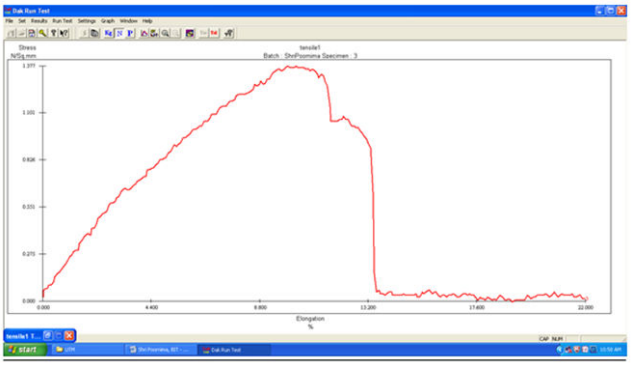

d

Figure 6d: Stress-Strain curve of CS-GG AgNP Film 3.

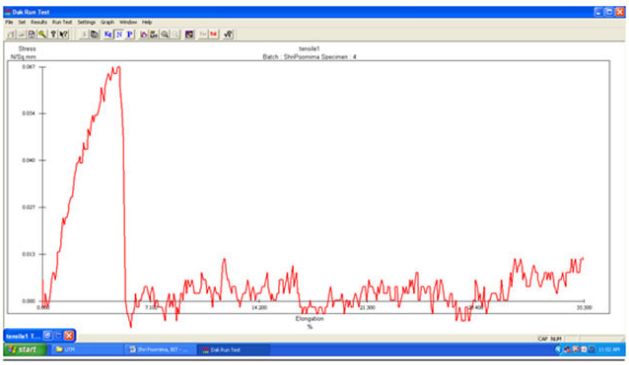

e

Figure 6e: Stress-Strain curve of CS-GG Sol.Blend Film 1.

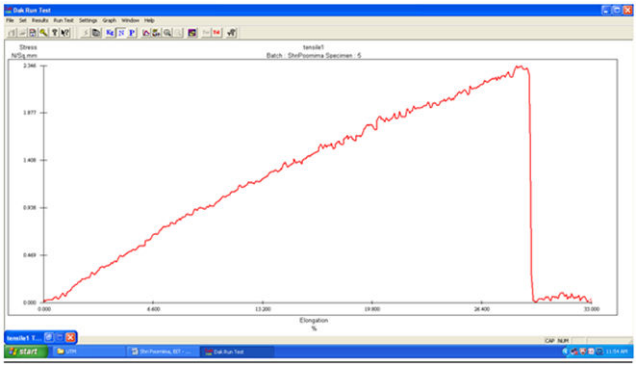

f

Figure 6f: Stress-Strain curve of CS-GG Sol.Blend Film 2.

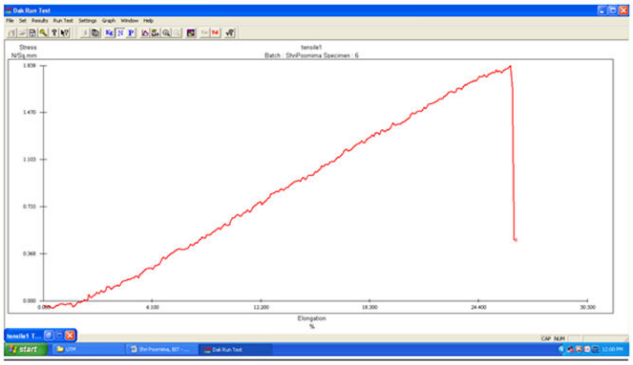

g

Figure 6g: Stress-Strain curve of CS-GG Sol.Blend Film 3.

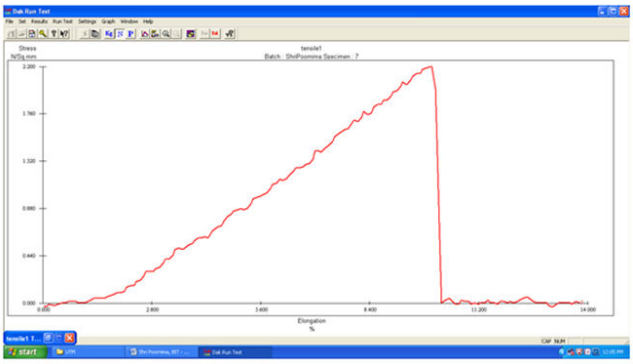

h

Figure 6h: Stress-Strain curve of CS-GG CuONP Film 1.

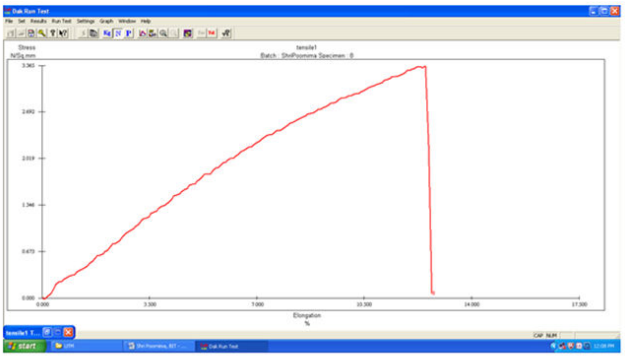

i

Figure 6i: Stress-Strain curve of CS-GG CuONP Film 2.

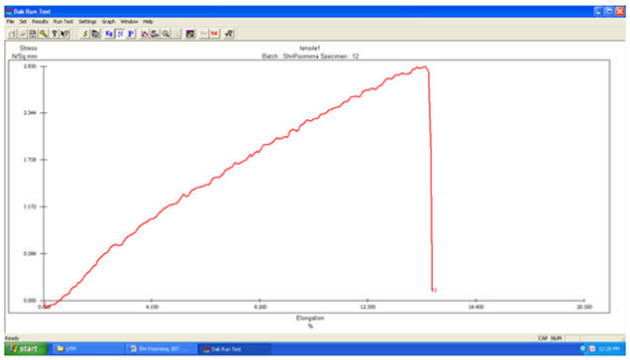

j

Figure 6j: Stress-Strain curve of CS-GG CuONP Film 3.

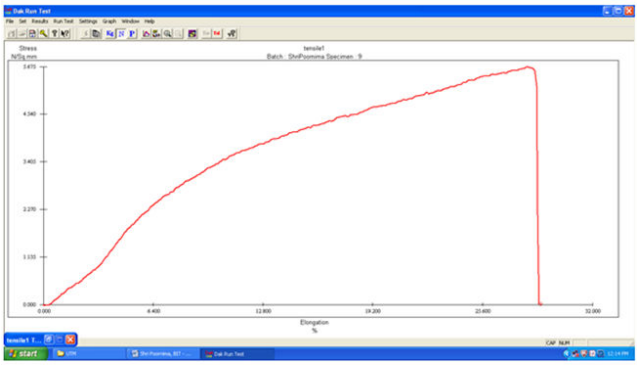

k

Figure 6k: Stress-Strain curve of CS-GG ZnONP Film 1.

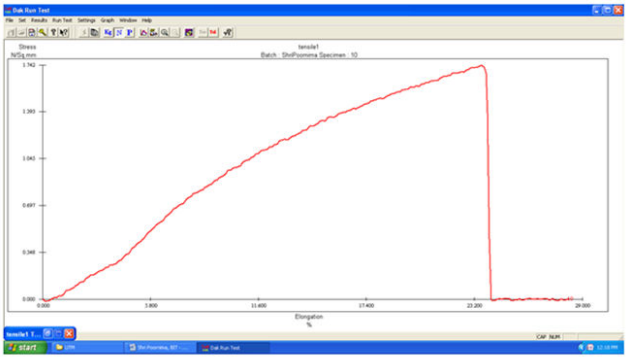

l

Figure 6l: Stress-Strain curve of CS-GG ZnONP Film 2.

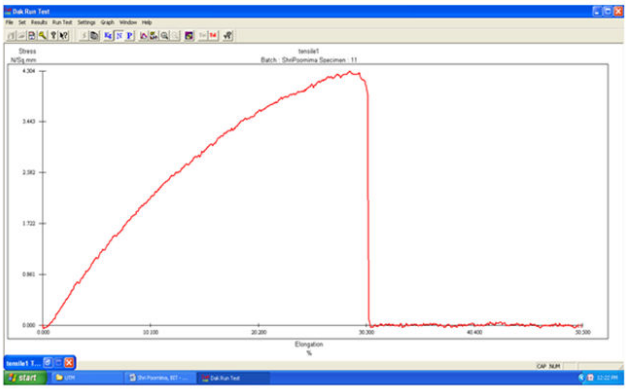

m

Figure 6m: Stress-Strain curve of CS-GG ZnONP Film 3.

Polymer film	Cross sectional surface area (mm^2)	Peak load (N)	Tensile strength N/ Sq.mm	Elongation break %	Modulus 10% N/ Sq.mm
CS-GG AgNP 1	1.5	3.9442	2.6295	24.6488	1.4013
CS-GG AgNP 2	1.25	2.5789	2.0631	26.6199	0.7531
CS-GG AgNP 3	1	1.3752	1.3752	11.5488	1.3702
CS-GG 1	5	0.3344	0.0669	5.0582	0.0022
CS-GG 2	1.25	2.9316	2.3453	29.2594	0.961
CS-GG 3	1.2	2.2039	1.8366	26.2	0.5708
CS-GG CuONP 1	0.75	1.6492	2.1989	9.9988	2.1964
CS-GG CuONP 2	1.15	3.8606	3.357	12.4988	2.9225
CS-GG CUONP 3	0.75	2.193	2.924	14.6	2.2576
CS-GG ZnONP 1	1	5.6749	5.6749	28.6488	3.333
CS-GG ZnONP 2	2.5	4.3533	1.7413	23.8488	0.9573
CS-GG ZnONP 3	0.75	3.227	4.3026	30.3988	2.1208

Table 1: Breaking load. The Tensile Strength (TS) and Elongation Break (EB) for CuONP, ZnONPs, AgNPs CS-GG films.

Moisture permeability and moisture absorption

The film's moisture resistance is also checked by packaging any materials, allowing it to resist water vapour into the film. The moisture content can be measured using the below formula:

$$MC\% = \frac{m_i - m_f}{m_i} \times 100$$

From Table 2, it is concluded that GG-CS Ag NP film has a lesser moisture content (5.124%) than the other films, making it a better material for packaging and other biomedical applications. Moreover, the GG-CS CuONP film (6.87%) and GG-CS ZnONP film (6.7%) also have a lesser weight percentage than the total polymer weight. Therefore, it can also be preferred for food packaging applications (Figure 7).

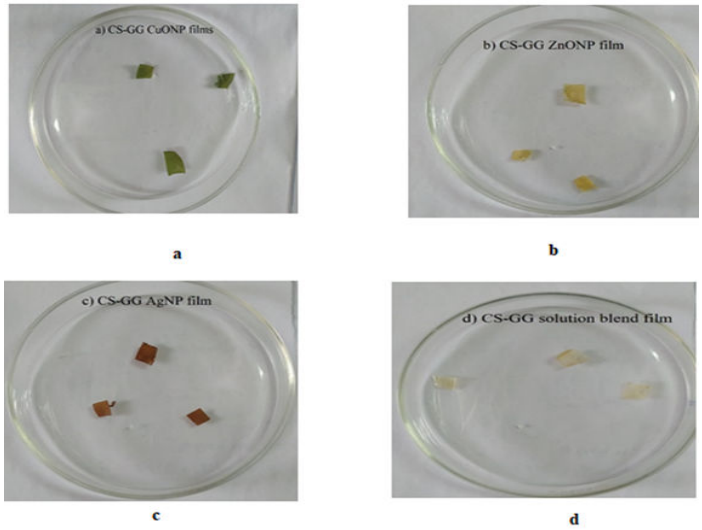

Figure 7: Water immersion test. a) CS-GG CuONP films in distilled water; b) CS-GG ZnONP films in distilled water; c) CS-GG AgNP films in distilled water; d) CS-GG CS-GG films in distilled water.

Polymer film with and without NP	Average of initial weight	Average of final weight	Weight % of moisture content	Weight % of moisture content with respect to polymer weight
GG-CS sol blend	0.00546 g	0.0066 g	17.27%	10.36%
GG-CS CuoNP film	0.0085 g	0.0096 g	11.46%	6.87%
GG-CS ZnONP film	0.01453 g	0.01636 g	11.18%	6.70%
GG-CS AgNP film	0.0121 g	0.01323 g	8.54%	5.12%

Table 2: Water immersion test. Moisture permeability and absorption of the CS-GG NP films.

Gobar gas degradability test

The film's degradation is also checked by placing the materials in cow dung treated distilled water and allowing it to degrade at three days intervals.

From Table 3, it is concluded that GG-CS Ag NP film has a greater degradation rate (10.9%) than the other films, making it a better material for packaging and other biomedical applications. Also, CS-GG Sol blend film also has a reasonable degradation rate (8.83%) compared to other films. The GG-CS CuONP film (4.8%) and GG-CS ZnONP film (6%) have a lesser weight percentage of degradation in comparison with total polymer weight. Therefore, it can also be preferred for food packaging applications. Hence the films are biodegradable and biocompatible for use in packaging applications (Table 3).

Polymer film with and without NP	Average of initial weight	Average of final weight	Weight % of degradation	Weight % of degradation with respect to polymer weight
GG-CS sol blend	0.00496 g	0.00423 g	14.71%	8.83%
GG-CS CuoNP film	0.0075 g	0.0069 g	8%	4.80%
GG-CS ZnONP film	0.0150 g	0.0135 g	10%	6%
GG-CS AgNP film	0.0110 g	0.0090 g	18.18%	10.90%

Table 3: Degradability test. Gobar gas degradation test for each bio nano composite films.

Conclusion

In the present study, the NP embedded composite polymer film was cast by solution casting successfully and characterized by XRD, SEM, FTIR, TGA, antimicrobial assay, structural stability in water and water vapour permeability. The polymer in the film showed an increased

amorphous feature in the presence of embedded NPs. The presence of NPS improved the tensile property of the film except in CuONP film. The latter was due to the poor dispersibility of NPs, as revealed by SEM pictures. There is no significant change in the onset degradation temperature of the NPS incorporated polymer films, but beyond the onset degradation temperature, the film displayed enhanced thermal stability. The zone of inhibition of *E. coli* and *B. subtilis* revealed that the bio nano composite films exhibited antimicrobial activity. The prepared nanoparticles embedded in polymer film showed structural stability on immersion in water and decreased water vapour permeability. These observed properties appeared promising for their applications in the packaging and biomedical field. The films have sufficient thermal stability for these applications. A mild decrease in the onset degradation temperature of NPs embedded polymer film turned out to imply that these composite films may biodegrade at a faster rate than those without metal and metal oxide NPs.

Acknowledgement

The authors are thankful to the management of Bannari Amman institute of technology for providing the necessary facilities to complete our research work. We also express our gratitude to Karunya institute of technology for providing us the facilities of X-RAY-Diffractometer SHIMADZU model XRD 6000 using Cu Ka radiation, Scanning Electron Microscopy (SEM) JEOL JSM 6390 and Kumaraguru college of technology for providing the facility of testing the breaking load using universal testing machine Dak Inc.

References

1. Souza VGL, Alves MM, Santos CF, Ribeiro IAC, Rodrigues C, et al. (2021) Biodegradable chitosan films with ZnO nanoparticles synthesized using food industry by products-production and characterization. Coat 11:646.
2. Mudgil D, Barak S, Khatkar BS (2014) Guar gum: Processing, properties and food applications A Review. J Food Sci Technol 51:409–418.
3. Sharma G, Sharma S, Kumar A, Al-Muhtaseb AH, Naushad M, et al. (2018) Guar gum and its composites as potential materials for diverse applications: A review. Carbohydr Polym 199:534–545.
4. Youssef AM, Assem FM, El-Sayed HS, El-Sayed SM, Elaaser M, et al. (2020) Synthesis and evaluation of eco-friendly carboxymethyl cellulose/polyvinyl alcohol/CuO nanocomposites and their use in coating processed cheese. RSC Adv 10:37857–37870.
5. Kraśniewska K, Galus S, Gniewosz M (2020) Biopolymers based materials containing silver nanoparticles as active packaging for food applications A review. Int J Mol Sci 21:698.
6. Xing Y, Li W, Wang Q, Li X, Xu Q, et al. (2019) Antimicrobial nanoparticles incorporated in edible coatings and films for the preservation of fruits and vegetables. Molecules 24:1695.
7. Shamhari MN, Wee SB, Chin FS, Kok YK (2018) Synthesis and Characterization of Zinc Oxide Nanoparticles with Small Particle Size Distribution. Acta chim Slov 65:578-585.
8. Sawle BD, Salimath B (2008) Biosynthesis and stabilization of Au and Au–Ag alloy nanoparticles by fungus, Fusarium semitectum. Sci and Technol Adv Mater 9:035012.
9. Sui C, Zhang W, Ye F, Liu X, Yu G (2016) Preparation, physical, and mechanical properties of soy protein isolate/guar gum composite films prepared by solution casting. J Appl Polym Sci 133.
10. Huq MA (2020) Green Synthesis of Silver Nanoparticles Using Pseudoduganella eburnea MAHUQ-39 and their Antimicrobial Mechanisms Investigation against Drug Resistant Human Pathogens. Int J Mol Sci 21:1510.
11. Jyoti K, Baunthiyal M, Singh A (2015) Science Direct Characterization of silver nanoparticles synthesized using Urtica dioica Linn. Leaves and their synergistic effects with antibiotics. J Radiat Res Appl Sci 9:217–227.
12. Ganachari SV, Bhat R, Deshpande R, Venkataraman A (2012) Extracellular biosynthesis of silver nanoparticles using fungi *Penicillium diversum and their antimicrobial activity studies*. Bio Nano Sci 2:316-321.
13. Awwad NS, Ali HE, Menazea AA (2022) Optical, thermal and dielectric properties of Copper Oxide (CuO)/chitosan (CS)/ Polyethylene oxide (PEO) blends. J Polym Res 29:177.
14. Senthilkumaar S, Rajendran K, Banerjee S, Chini TK, Sengodan V (2008) Materials Science in Semiconductor Processing Influence of Mn doping on the microstructure and optical property of ZnO. Mater Sci Semicond Process 11:6–12.
15. Elango M, Deepa M, Subramanian R, Musthafa AM (2017) Synthesis, Characterization and Antibacterial Activity of Polyindole/Ag–Cuo Nanocomposites by Reflux Condensation Method. Polym Plast Technol Eng 0:1–12.
16. El-nahhal IM, Salem J, Anbar R, Kodeh FS, Elmanama A (2020) Preparation and antimicrobial activity of ZnO-NPs coated cotton/ starch and their functionalized ZnO-Ag/cotton and Zn (II) curcumin/cotton materials. Sci Rep 10: 1–10.
17. Asamoah RB, Annan E, Mensah B, Nbelayim P, Apalangya V, et al. (2020) A Comparative Study of Antibacterial Activity of CuO/Ag and ZnO/Ag Nanocomposites. Adv Mater Sci Eng 2020.
18. Li K, Jin S, Liu X, Chen H, He J, et al. (2017) Preparation and characterization of chitosan/soy protein isolate nanocomposite film reinforced by Cu nanoclusters. Polym 9:247.
19. Patel M (2022) Synthesis of ZnO and CuO nanoparticles *via* Sol-gel method and Its Characterization using XRD and FT-IR analysis. Discov Mater 2:1-1.
20. Muhammad W, Ullah N, Haroon M, Abbasi BH (2019) Optical, morphological and biological analysis of Zinc Oxide Nanoparticles (ZnO NPs) using Papaver. RSC Adv 9:29541-29548.